Mars Mission Applications Enabled by a High-Power Solar Electric Propulsion (SEP) Power and Propulsion Element (PPE)

Melissa L McGuire,* David A Smith†,
Maya N Havens‡, Steven R Oleson,§ Elizabeth R Turnbull**
NASA Glenn Research Center, 21000 Brookpark Road, Cleveland, OH, 44135

With the culmination of years of research and development in space solar power and electric propulsion systems, NASA and its partner Lanteris Space Systems (formerly Maxar Space Systems) are designing and building a high-power SEP Stage called the Power and Propulsion Element (PPE).[1] High power Solar Electric Propulsion (SEP) systems can enable a wide range of exploration missions, both human and robotic. In its specific application, the PPE is being designed to provide power and propulsion for Gateway, an orbital platform that will support long-term exploration missions on the moon's surface, as part of NASA's Artemis program. The high power SEP system on PPE will support lunar exploration missions and enable future missions through this capability. This paper will examine the applicability of a high-power SEP system similar to the PPE's specifications to a series of Mars mission concepts designed by NASA Glenn's Concurrent Engineering Compass team, including its usage as both a spacecraft and a payload delivery vehicle.

I. Introduction

In cases where time is not a critical factor in the transit of the payload, Solar Electric Propulsion (SEP) has enabled the efficient delivery of science and robotic payloads to planetary destinations for reduced propellant costs when compared to high thrust chemical propulsion systems. Being developed to enable solar system exploration, NASA will use the high-power SEP Power and Propulsion Element to deliver and maintain the Gateway orbital platform in a semi-stable orbit around the moon[2]. When it flies, the PPE will demonstrate an SEP system about ten times more powerful than any previously flown, enabling delivery of much larger payloads to the Moon on a single launch than previously achieved. This efficient electric propulsion system is an important step in the development of high-power vehicles that will enable human exploration to Mars and previously impossible robotic exploration to the outer planets.

Inspired by the high power and efficient propulsive capabilities of the PPE, the PPE Mission Design team collaborated with the NASA Glenn Research Center's Compass team to apply a PPE class SEP spacecraft to Mars mission concepts. Due to its high-performance SEP system, a PPE class spacecraft is well suited to Mars mission applications. The high-power solar arrays combined with electric thruster systems are capable of delivering large payloads and providing significant power to science and other instruments while in Mars orbit. This paper captures the four mission concept designs, details of the trajectory trades, and preliminary assessments of eclipses and communications links completed in the Compass study.

* PPE Mission Design Lead, LSM/Mission Architecture and Analysis Branch, NASA GRC.
† PPE Mission Design Engineer, LSM/Mission Architecture and Analysis Branch, HX-5.
‡ PPE Mission Design Engineer, LSM/Mission Architecture and Analysis Branch, NASA GRC.
§ Compass Team Lead, LSM/Mission Architecture and Analysis Branch, NASA GRC.
** Compass Lead Systems Engineer, LSM/Mission Architecture and Analysis Branch, NASA GRC.

II. Compass Team Background

Established in 2006 at NASA Glenn Research Center[3], the Compass team is a multidisciplinary, concurrent engineering design team whose primary purpose is to perform rapid integrated systems analysis for space-based missions.[4] Working in real time with inputs from the various disciplines in a Compass session, a vehicle concept can come together rapidly and evolve in a very efficient manner to produce a design that achieves the customer's goals. The engineering discipline leads are matrixed in from different organizations across the center. For this study session, PPE Systems Engineering and Integration, Mission Design, and Safety and Mission Assurance were embedded into the Compass team and acted as customers for the concept designs.

III. Ground Rules and Assumptions

As much as was possible, all inputs used in the ground rules and assumptions for this design were derived from publicly available information about the PPE. Due to the fact that the PPE was contracted as a public private partnership, much of the specific details of the PPE are competition or otherwise sensitive and where those data cannot be shared, approximations were made.

For the four concept examples discussed here, the Compass design assumed the use of a Falcon Heavy Expendable (FHE) launch vehicle to deliver the PPE and Payload to escape and applied performance data that is publicly available from the NASA Launch Services Program Launch Vehicle Performance Website.[5] A variant fifth concept not documented here assumed a reuseable Falcon H and decreased the ΔV performed by the launch vehicle and increased the ΔV performed by the PPE in interplanetary space to reach the destination Mars orbit.

The PPE is a 50-kW class high-power SEP stage comprised of two different types of electric thruster strings, Advanced Electric Propulsion System (AEPS) and Busek's BHT-6000[6]. To both maximize the final delivered mass and attempt to minimize the time spent in the Van Allen Belts early in the transit trajectory, the EP system is operated in two different modes, a high-thrust mode to reduce trip time early in the trajectory and a high-Isp (specific impulse) mode later in the trajectory to conserve propellant. Compass design study assumed the use of only the high-power 13.1 kW Hall effect AEPS thrusters to perform the interplanetary transit and Mars orbit insertion.[7] The number of thrusters (1-3) used was dependent on the available power, which decreased with the inverse square of the distance from the sun ($1/R^2$).

For the spacecraft bus, the concept designs used the PPE as-is as much as possible. For example, since a PPE application at Mars would not require the orbit maintenance of the lunar-orbiting Gateway, the PPE for Mars concepts were able to off-load chemical propellant.

IV. Mars Concept Case Overview

The Compass 40 kW class SEP-for-Mars study created four concept designs, shown in Figure 1, each with a slightly different focus at Mars. The cases varied, trading trip time to Mars for performance to C_3. Higher C_3 departure from the launch vehicle results in less mass thrown to a higher energy escape trajectory, leaving less of the remaining delta V for the trip to Mars performed by the on-board SEP system. Case 1 focused on trip time at the expense of mass delivered to Mars. In the remaining three cases, the SEP system was able to deliver more mass to Mars as it did more of the interplanetary delta-V, at the expense of trip time.

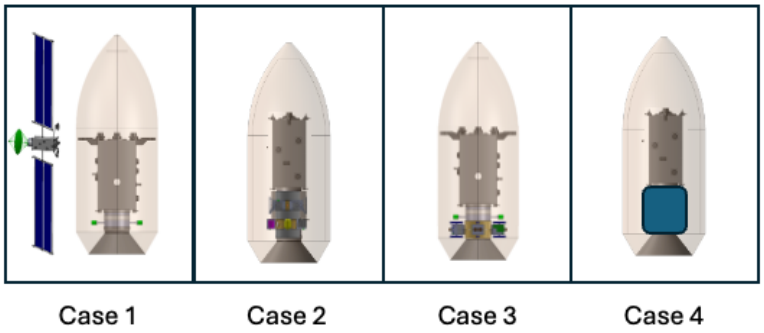

Figure 1. PPE to Mars Concept Designs shown in their stowed configuration in the FHE fairing.

V. Trajectory Design Overview

This study evaluates a Solar Electric Propulsion (SEP) mission concept for a modified Power and Propulsion Element (PPE) class spacecraft performing an interplanetary transfer from Earth to Mars. The analysis uses the Copernicus trajectory optimization software[8] to explore four trajectory cases that trade total mission duration for delivered payload mass[9]. Including the Mars orbital spiral, total mission durations range from approximately 800 to 1100 days.

A high-level schematic of the trajectory model is shown in Figure 2. The process begins with launch performance from the Falcon Heavy Expendable (FHE) launch vehicle, which defines the injected mass and launch C_3 at Earth departure. The total SEP wet mass is constrained by the FHE payload curve, reduced by 10% to reserve margin. This constraint is embedded in Copernicus via plug-ins that allow optimization over both mass and C_3 while remaining compliant with launch capability.

The heliocentric phase begins at Earth escape and ends at Mars arrival, defined by Mars $C_3 = 0$ km²/s². Post-arrival low-thrust spirals to operational orbits are not explicitly modeled within the transfer but are incorporated through ΔV estimates drawn from prior Copernicus analyses and a modified version of OTIS (Optimal Trajectory by Implicit Simulation)[10]. These estimates enable accurate calculation of final delivered mass and time-to-operational orbit following capture. The spiral ΔVs assume in-plane targeting of the final Mars orbit with no plane change. This implies that the correct inclination at Mars is targeted during the interplanetary transfer. The one exception to this spiral assumption is a single case studied where the spacecraft first targets the orbit of Deimos and then completes a transfer to Areosynchronous orbit (ASO) requiring the ΔV to account for a small plane change on the order of ~1°.

All modeled transfers use a burn–coast–burn profile. A mandatory 30-day coast phase is inserted immediately following Earth departure to support spacecraft checkout and commissioning. In faster trajectories approaching continuous propulsion, additional mid-course coasts of 10–15 days are added to reflect realistic operational constraints.

The propulsion model supports dynamic engine-mode switching within each thrust arc, allowing Copernicus to select among single-, dual-, or triple-engine modes based on real-time power availability. A 90% duty cycle is applied to account for eclipses, communications cutouts and system-level transitions.

It is assumed that the power system provides 60 kW at 1 AU, degrading with distance via a simple $1/R^2$ relationship. Beginning-of-life (BOL) performance is assumed constant throughout the mission, with no time dependent array degradation modeled.

The spacecraft departs Earth with 2.770 metric tons of xenon propellant[11] which is a not to exceed value in the execution of the mars transfer and insertion. (Excess propellent is permitted at the end of the transfer and subtracted from any final mass when determining "payload"). Optimization objectives include maximizing delivered mass to Mars orbit, minimizing propellant consumption, or minimizing transfer time for a fixed delivery target.

Outputs from Copernicus—such as departure and arrival dates, ΔV requirements, propellant usage, and time of flight—serve as inputs for iterative spacecraft design refinement and are central to developing a robust architecture for the planned 2028 Earth–Mars transfer opportunity.

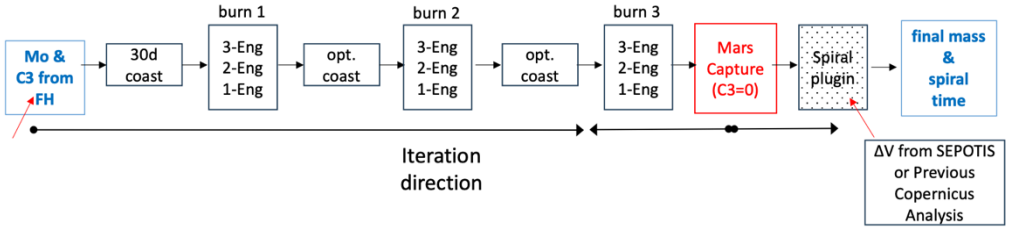

Figure 2. Copernicus mission design model flow.

As shown in Figure 2, the trajectory is designed with alternating, optimal length coast and burn arcs with options for engine switching (optimizer selected). Launch C_3 and wet mass are constrained by FHE performance (dark blue is published payload while the light blue represents payload with 10% mass reserve). Mars spiral ΔV and timing are incorporated post-capture via plug-in, using data from OTIS or prior Copernicus runs. Although the second burn and coast arcs were not used in the results presented in this paper, they remain in the model architecture to support potential future mission scenarios.

Table 1 summarizes the per-engine thrust, mass flow rate, and specific impulse (Isp) for a single AEPS thruster string as a function of power input to the Power Processing Unit (PPU)[6]. Data values for input powers range from 10 to 13.3 kW. At full power (13.3 kW), a single AEPS thruster produces 0.579 N of thrust with a specific impulse of 2600 seconds and a mass flow rate of 2.271×10^{-5} kg/s.[12].

Table 1. Per-engine performance characteristics of AEPS[6].

# eng	1		
AEPS Per Engine Performance (1 engines)			
input pwr (kW)	**Thrust (N)**	**mdot (kg/s)**	**Isp (s)**
13.3	**0.579**	2.271E-05	2600
13.0	**0.576**	2.269E-05	2588
12.0	**0.546**	2.250E-05	2474
11.0	**0.517**	2.235E-05	2359
10.0	**0.488**	2.217E-05	2244

These thrust and mass flow data were curve-fit and scaled to model one, two, or three AEPS thrusters. The resulting performance maps were implemented into Copernicus as parametric engine models, constrained by user-defined power availability. The system assumes a 90% duty cycle, and any available power beyond the operational maximum is treated as "shunted," meaning it does not contribute to thrust. Conversely, if the available power drops below the minimum operating threshold, the thruster is shut down entirely.

Solar power availability was modeled using a $1/R^2$ scaling law and assumed a nominal power of 60 kW at 1 AU (Earth). At Mars (1.66 AU), this corresponds to a pre-bus power availability of approximately 20.7

kW. Bus power for the entire study was assumed to be 4kW. Accounting for spacecraft bus loads, the power available to propulsion during the Earth to Mars transfer phase ranges between 16 and 23 kW, depending on heliocentric distance. Because there exists a specific, minimum amount of power required to operate two of the AEPS thrusters simultaneously, the baseline trajectory analysis conservatively assumes a single thruster operating at full power throughout the spiral descent at Mars. This approach maximizes propellant efficiency while providing conservative estimates of time of flight.

The optimal trajectory solution uses one-, two-, or three-engine thrust and mass flow curves at each point in the trajectory as needed, based on the available power and mission design objectives. This flexibility is maintained across all burn arcs, where the optimal segment durations are selected—ranging from 0 seconds to effectively continuous thrusting—to allocate the appropriate engine configuration and maximize performance within operational constraints.

VI. Mars Concept Cases Trajectory Design Results

This section presents four distinct trajectory and payload delivery cases designed to explore the trade space of solar electric propulsion (SEP) transfers from Earth to a designated operational orbit around Mars. Each case begins with launch aboard a FHE vehicle and employs a common transfer architecture—comprising an Earth–Mars interplanetary leg followed by a low-thrust descent phase into Mars orbit. The cases differ primarily in their mission design objectives, targeting various combinations of transfer duration, delivered mass, and orbital insertion strategy. Each case is discussed in detail in its own subsection. In order to protect the sensitive nature of the PPE specific data, launch C_3 (energy) and departure mass are not reported in this paper. Only the ΔV values optimized for the interplanetary trajectory or estimated for the final orbit insertions and delivered payload mass are reported.

Case 1: This case was a "fast transfer" from Earth escape to Areosynchronous orbit (ASO), targeting a brief pass through the orbital region of Mars' moon Deimos. Designed to minimize time of flight, the delivered mass was a result of the propellant required to complete the transfer. The ΔV values used at insertion were 1,100 m/s from Mars SOI to Deimos and 150 m/s from Deimos to ASO. The 150 m/s ΔV value accounts for the small plane change associated with this segment.

The trajectory, shown in Figure 3a, departs Earth on 18 December 2028, captures at Mars on 14 February 2030, and arrives in ASO 25 days later resulting in a total transfer time of approximately 633 days. The trajectory is characterized by its nearly all-propulsive nature, optimizing departure and arrival dates to avoid unnecessary coasting.

This case resulted in the highest departure C_3 of the four cases. Stay time at Deimos was not modeled. Thruster off-time due to eclipses was not explicitly modeled beyond the 10% duty cycle assumption. However, eclipse durations at the high altitude of ASO (~17,000 km) are expected to be minimal and can be addressed through mission planning if necessary.

Due to the high C_3 and low escape mass, the delivered payload was limited to a ~300 kg Mars science package. This enabled the Compass team to design a UHF relay payload with a deployable antenna with X-band DTE capability. Despite the small payload, the system supports high data return rates and modest power requirements.

Case 2: This case was optimized for maximum delivered mass and targets a 5-sol-synchronized orbit. The trajectory is shown in Figure 3b. Earth departure occurred on 19 July 2028 with Mars capture on 24 October 2030. The subsequent spiral descent to the final orbit required approximately 154 days, with orbital insertion occurring on 27 March 2031. Total mission duration was 980 days.

This case used a much lower C_3 than Case 1. The ΔV for the Mars spiral segment was set to 640 m/s. The Earth–Mars transfer required 4.6 km/s of ΔV.

The final delivered payload was approximately 4 metric tons. The resulting Compass design assumed long-duration science operations (up to five years) and benefited from a higher power allocation (up to 15 kW), although with lower expected data return rates.

Case 3: This case is like Case 1 in that it also targeted Deimos and ASO using a minimum-time-of-flight objective. However, unlike Case 1, the final payload mass was fixed at 2 metric tons rather than being left open for optimization. This constraint significantly altered the transfer profile, as illustrated in Figure 3c. Spiral ΔV assumptions at Mars matched those used in Case 1.

Earth departure occurred on 20 September 2028, with Mars capture on 27 March 2030 and arrival in ASO 240 days later on 24 November 2030. Despite the time-minimization objective, the total mission duration was approximately 795 days—longer than Case 1 due to the heavier payload requirement.

Earth escape was characterized by a moderate C_3. Both three- and two-engine thrust arcs were employed to move this larger mass. The Earth–Mars transfer required nearly 5 km/s of ΔV. The spiral maneuver to arrive in the final desired orbit required additional propellant than that required in Case 1.

The Compass team designed the delivered payload to include multiple deployable smallsats and a shared UHF relay. Although lighter than Case 2, this configuration preserved high data return rates and moderate power demands while supporting distributed science operations.

Case 4: Like Case 3, this case targeted a 2 metric ton payload with a minimum-time objective. However, the final orbit was a low Mars orbit (LMO) instead of ASO. The interplanetary transfer followed the same structural configuration as in the other cases but required a significantly larger ΔV for the spiral descent—estimated at 3 km/s using OTIS with comparable mass and propulsion assumptions. The resulting trajectory is presented in Figure 3d.

Earth departure occurred around 15 October 2028, with Mars capture on 12 March 2030 and LMO insertion on 28 September 2031. The total transfer duration was 1,078 days, the longest of all four cases. The interplanetary segment required 3.9 km/s of ΔV.

The payload for this case was a ~2 metric ton radar instrument package, designed by the Compass team for long-duration science operations. The system supports up to 10 kW of power and moderate data return rates tailored for synthetic aperture radar or similar remote sensing instruments.

Overall Observations: As expected, mission C_3 varies as a function of payload mass and transfer duration. Lower C_3 values generally correspond to longer transfer times and higher delivered mass. Power and data return capabilities also reflect tradeoffs between payload type, orbital altitude, and operational lifespan.

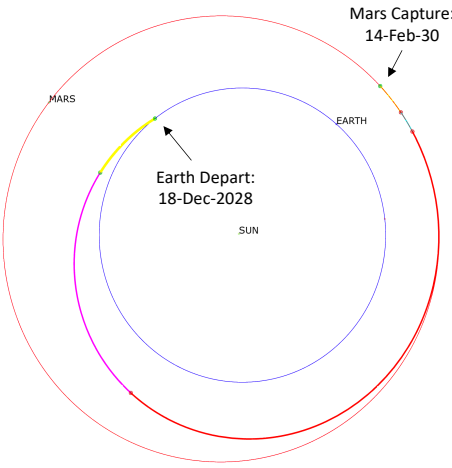

Figure 3a. Case 1 - minimum time to ASO

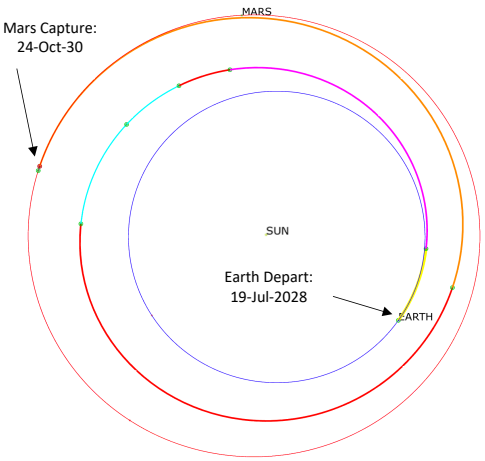

Figure 3b. Case 2 - maximum mass to 5-sol

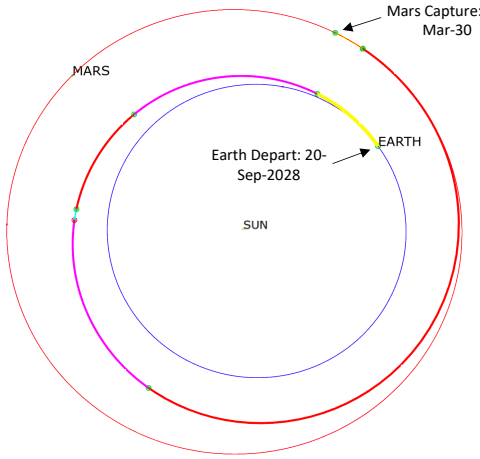

Figure 3c. Case 3 - minimum time, 2t to ASO

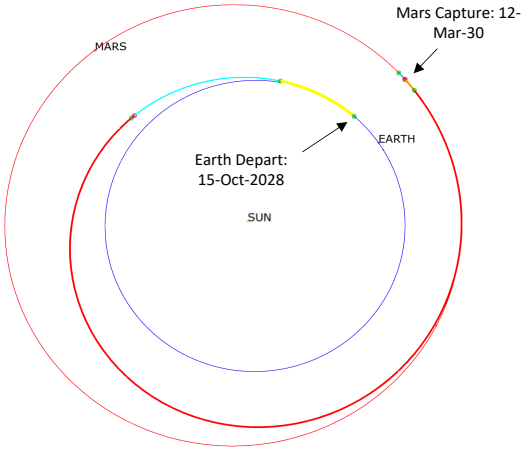

Figure 3d. Case 4 - minimum time, 2t to LMO

Figure 3. Copernicus-modeled heliocentric Earth-to-Mars (SOI) transfer. Three-, two-, and one-engine thrust arcs are depicted in magenta, red, and orange respectively. Forced and optimal coast periods are shown in yellow and light blue, respectively.

VII. Parametric Sweep of Earth Departure and Transfer Duration

To extend the analysis of Case 2 (the 5-sol mission), a parametric sweep was performed to evaluate the maximum delivered mass as a function of Earth departure date and time of flight (ToF). Each point on the grid corresponds to a separate trajectory solution, computed by optimizing the departure state to lie on the FHE payload performance curve for a fixed launch date and ToF. The Earth departure dates span the years 2028 to 2036, while ToF values range from 2.0 to 3.0 years. The grid was evaluated on a month-by-month basis using a 16-core parallel computing setup and required slightly more than one week to converge. The optimization process used seeding, where neighboring points were initialized with solutions from recently

converged cases, and already converged cases were periodically re-optimized to detect further improvements. Iterations continued until convergence ceased to improve.

Maximum delivered mass is shown in Figure 4 as a function of Earth departure date and ToF for a FHE launch and low-thrust Mars transfer. Each cell represents an individually optimized trajectory solution. Delivered mass combines dry mass, payload, and any excess propellant. The plot reveals that favorable Earth–Mars transfer opportunities occur in roughly 26-month synodic intervals, with primary windows in 2028, 2030/31, 2033, and 2035. The most advantageous launch period appears in 2028, producing delivered masses exceeding 10 metric tons for a wide range of ToFs. In contrast, alternate years within the synodic cycle generally yield reduced delivered mass potential, often in the 6–7 metric ton range, and exhibit fewer converged cases, especially at shorter ToFs. In all cases, it can be observed that SEP delivers notable payload to Mars even in the less favorable years.

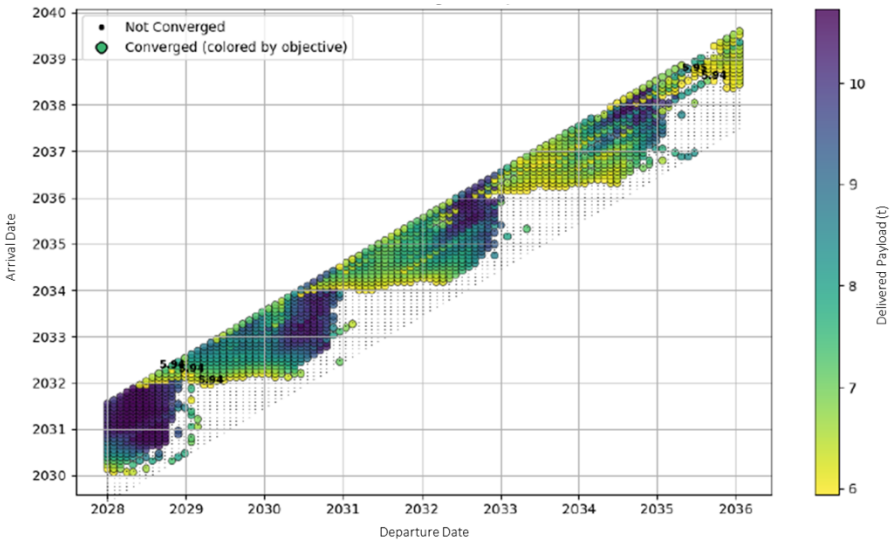

Figure 4. Maximized objective payload: delivered mass (metric tons) for arrival date at Mars shown as a function of Earth departure date.

VIII. Eclipse and Communication Line-of-Sight Analysis

The PPE is designed to be thermally resilient to eclipses of no longer than 90 minutes in duration. This is accomplished in the Gateway mission through the design of the destination NRHO and along the lunar transit by careful trajectory design. Visibility to the Sun is crucial both to ensure reliable power generation and periods of eclipse not to exceed the Power and Propulsion Element's (PPE) maximum eclipse requirement of 90 minutes. An assessment was done to establish the eclipse durations and locations during a Mars mission for a notional Mars orbiter over a five-year period from 2025 to 2030. The two Mars orbits that a notional PPE derived vehicle was assessed in were a 5-sol orbit around Mars and an Areosynchronous orbit positioned above the Jezero crater.

Visibility to Earth and the Jezero Crater is essential for maintaining real-time communications. Additional analysis of this notional PPE derived vehicle as a potential Mars communication link focused on the line-of-sight between the spacecraft in either of the two Mars orbits assessed for eclipses and the Jezero Crater on Mars (where a lander would be notionally located) and the Earth. The results of these analyses will be discussed below.

A. Eclipse Analysis

The eclipse periods occurring when Mars blocks the line-of-sight of the Areosynchronous orbiter to the Sun are shown in Figure 5. The horizontal dashed red line represents the PPE 90-minute maximum eclipse requirement. The vertical dashed orange and green lines represent the dates of the Mars Northern Autumn and Spring equinoxes, respectively. The behavior is periodic, with two eclipse seasons centered around the Mars northern spring and autumn equinoxes. The shortest time seen between eclipse seasons is around 218 days, with the longest time between eclipse seasons being around 289 days. Within an eclipse season, eclipses occur around once a day.

The shortest eclipse duration observed was ~1 minute, while the maximum eclipse observed was ~1.3 hours. All eclipses observed by the Areosynchronous orbiter fall well within the Power and Propulsion Element (PPE) maximum eclipse requirement of 90 minutes. This behavior makes the Areosynchronous orbit a reliable option.

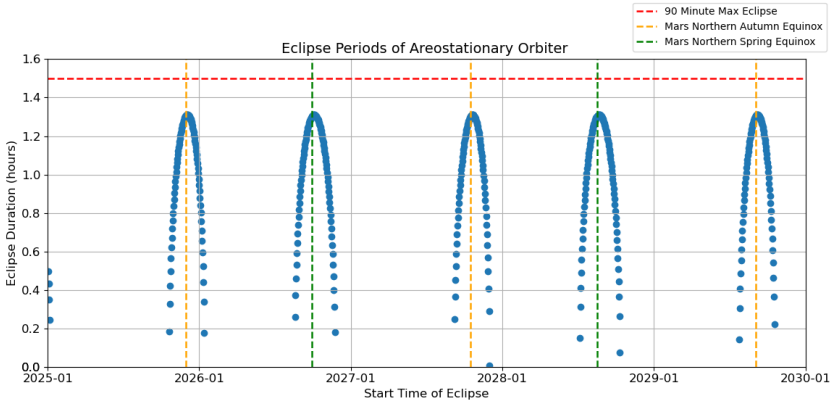

Figure 5. Eclipse periods of Areosynchronous orbiter from 2025 to 2030.

Like the Areostationary orbiter, the 5-Sol orbiter experiences seasons of eclipses during certain parts of the year as shown in Figure 6. The shortest time seen between eclipse seasons (excluding the 3 outliers) is around 237 days, with the longest time between eclipse seasons being around 370 days. Within an eclipse season, eclipses occur around once every 5 sols, or 5.1 days. The shortest eclipse duration observed was 4 minutes, while the maximum was 8.3 hours.

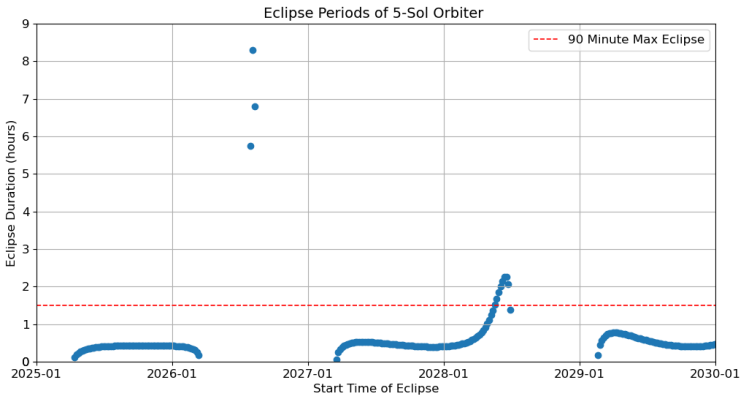

Figure 6. Eclipse periods of 5-Sol orbiter from 2025 to 2030.

Short eclipses typically occur at periapsis as shown in Figure 7, with the outliers halfway into 2026 caused by poor alignment, as shown in Figure 8. Though most of the eclipses observed by the 5-Sol orbiter are within the PPE maximum eclipse requirement of 90 minutes, there are some that exceed the requirement. To combat this, careful mission planning and re-phasing could be done to shift the Right Ascension of the ascending node (RAAN) of the orbit to avoid long eclipses.

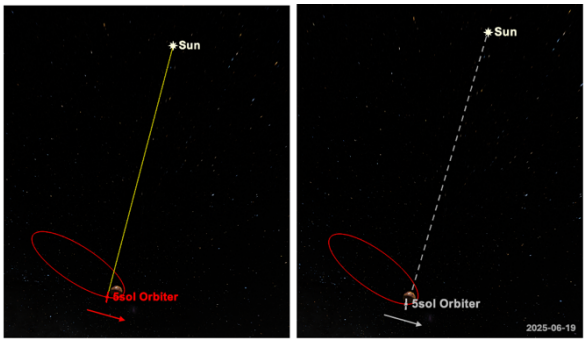

Figure 7. Typical short-duration 5-Sol eclipse occurring at periapsis passage.

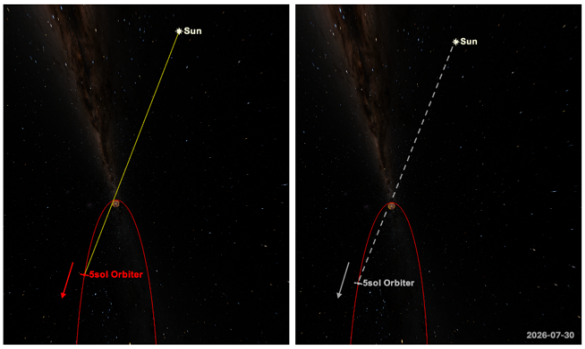

Figure 8. Outlier 5-Sol eclipse caused by poor alignment.

A preliminary examination of the eclipse patterns in both the Areosynchronous and 5-Sol orbits at Mars indicate that each Mars orbit option is within the design boundaries of a PPE derived spacecraft for certain time periods. Any long eclipses could be avoided with careful mission planning.

B. Communications Line-of-Sight Analysis

Lastly, the Compass team did a preliminary assessment of line-of-sight communications between the PPE derived vehicle in each of the Mars orbit options, and Jezero crater and the Earth.

The Areosynchronous orbit is configured for constant visibility of the Jezero crater, outages for real-time communications are mostly dependent on the orbiter's visibility to Earth (shown in Figure 9). Daily outages occur in clusters with the minimum time of 173 days and maximum time of 409 days between clusters. There are two outliers in the dataset, one occurring about halfway into 2025 as the Earth's moon blocks visibility between the orbiter and Earth and another occurring in December of 2025 as a very brief 15 second outage, caused by Mars' moon Phobos as shown in Figure 10 and Figure 11. The longest outage observed over the period of analysis was 1.3 hours.

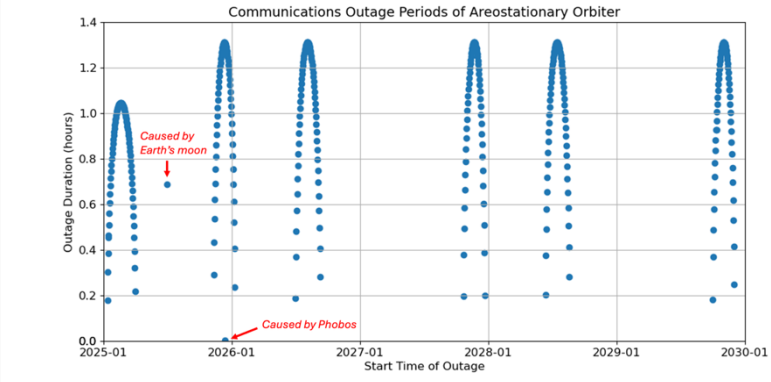

Figure 9. Communications outage periods of Areosynchronous orbiter from 2025 to 2030. Outliers and their causes are notated in red on the figure.

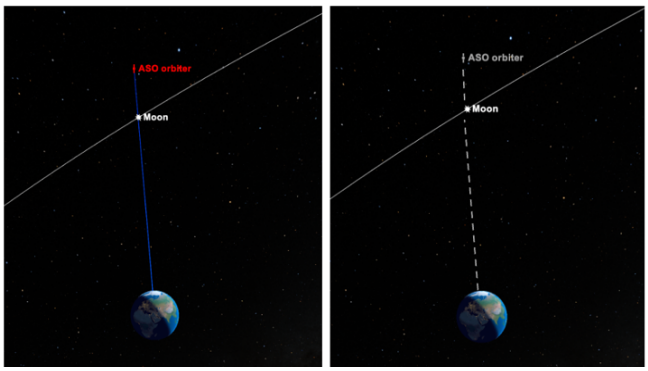

Figure 10. Outlier Areosynchronous communications outage caused by Earth's moon.

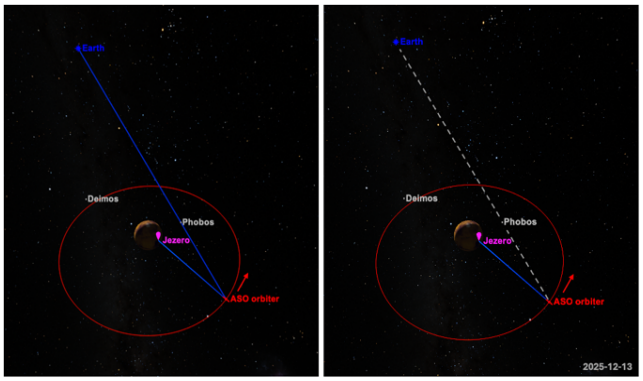

Figure 11. Outlier Areosynchronous communications outage caused by Mars' moon Phobos.

For the 5-sol orbit option, real-time communication capability is dependent on visibility to both the Jezero Crater and to Earth. Given the 5-sol orbiter's highly eccentric, long-period orbit, maintaining continuous visibility to both Jezero Crater and Earth presents unique challenges. Figure 12 shows real-time communications outages where the orbiter lacks visibility to both the Earth and Jezero crater simultaneously. The shortest outage observed over the period of analysis was about 7 minutes while the longest outage was 19.1 hours. The gap between these outages on average was 13 hours, with a minimum of 1 minute and a maximum of 15.8 hours.

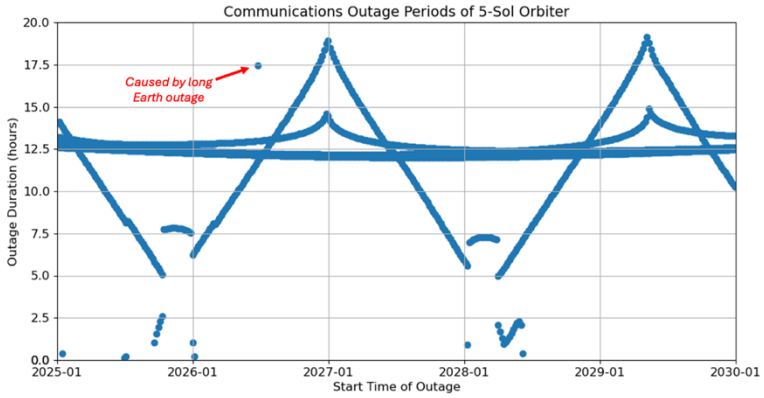

Figure 12. Real-time communications outage periods from 2025 to 2030, where the 5-Sol orbiter has communication with neither Earth nor the Jezero crater.

Consistent outages lasting approximately 12.3 hours occur when the orbiter is near apoapsis, aligning with half of Mars' rotational period when Jezero Crater faces away from the orbiter, resulting in communication disruptions. Near periapsis, outage durations vary depending on the alignment of Jezero Crater with the orbiter. If Jezero Crater is well-aligned with the orbiter during periapsis passage, a longer period of uninterrupted communication is possible. However, poor alignment can result in an extended communication outage.

Examination of both Mars orbit options indicate that either could be used as the location of a Mars relay satellite. The Areosynchronous orbit offers real time communications with further analysis needed on the 5-sol option if continuous communications between Jezero crater and the Earth is desired.

IX. Mars application concept designs

The four cases designed by the Compass team illustrate the range of design options available within a consistent SEP-based transfer framework. Table 2 summarizes the key parameters and outcomes of each case, providing a side-by-side comparison of launch dates, transfer durations, delivered masses, orbital targets, and associated ΔV requirements. This overview highlights the tradeoffs inherent in optimizing for time of flight, payload mass, or orbital geometry in future Mars missions using low-thrust propulsion.

Table 2. Summary of High Power SEP Mars Application Compass Concept Designs.

Details	Case 1	Case 2	Case 3	Case 4
Launcher	Falcon H Expendable	Falcon H Expendable	Falcon H Expendable	Falcon H Expendable
Mission	Launch to escape, spiral to Mars SOI, spiral down to ASO	Launch to escape, spiral to Mars SOI, spiral down to 5 SOL, support ~5t payload for ~ 5yrs	Launch to escape, spiral to Mars SOI, spiral down to ASO (visit Deimos on the way): deploy ~4 smallsats at ASO or Deimos (carry 2.5t)	Launch to escape, spiral to Mars SOI, spiral down to LMO, support ~2t radarsat payload for ~ 5yrs
Trip time to operations orbit	633 Days	980 Days	795 Days	1,078 Days
Payload Mass	~300 kg	~4t	~ 2.5t	2t
Payload Type	Mars science UHF relay plus X-band DTE with Deployable 5m antenna to 70m DSN, carry SIMPLEX-class ride-along to launch	5 Sol payload ESPA grande, carry SIMPLEX-class ridealong	(136kg) ESPA ring and four ~450 kg small sats for ASO or Deimos, ~300 kg Mars science UHF relay plus X-band DTE with Deployable 5m antenna	~Radarsat Payload
Power to Payload	~ 1 kW	~ 15 kW	~ 1kW	Up to 10 kW

These four Mars concept cases show the tradeoff between the use of the high thrust Falcon H and the low thrust PPE derived SEP system. Case 1, which relied on the FHE to deliver the PPE class spacecraft to a relatively high C_3, delivers a ~ 300 kg payload to Mars. Conversely, in Case 2, where the FHE delivers the PPE class spacecraft to a much lower escape C_3, utilized the efficient low thrust SEP system to deliver an order of magnitude more mass ~ 4000 kg to Mars orbit. As is typical of low thrust missions, the larger mass is achieved at the expense of longer trip time to the final Mars orbit.

X. CONCLUSION

The Compass design study concluded that a high-power PPE class SEP spacecraft, can deliver substantial payloads and function effectively at Mars, despite its distance from the sun. The PPE's large solar arrays can generate power sufficient to both perform the transit to Mars and to support the operation of various payload mission concepts once at Mars. Designs showed that the assumed PPE Xenon propellant capacity was sufficient to deliver a PPE class vehicle and a range of payload masses to Mars for most of the envisioned concept Mars missions. Further, the 90 minute eclipse thermal design assumptions of the PPE are satisfied in the potential operational Mars orbits examined. Onboard RCS bipropellant chemical load was only used minimally in the trajectory designs, but because the PPE has both Xenon and bipropellant on board, future work should investigate demonstrating SEP-Chem pre-cursor missions to Mars[13]. Due to Mars's colder environment Compass' rough analysis showed current PPE thermal design may need additional heaters at Mars and should consider either the addition of MLI to crucial components and/or louvers on the radiators. Additionally, care should be taken in the selection of operating orbits at Mars and potential phasing approaches to avoid potential long-duration eclipses which would negatively impact PPE systems. Future work should include implementing these changes to investigate the effect to the mission.

Overall, it can be seen from these preliminary results that a notional PPE derived 40-50 kW-class SEP spacecraft, with some modifications from its lunar Gateway application, can enable a wide variety of exploration mission supporting functions ranging from technology demonstrations to communications support to science applications. The Mars application demonstrated here by the Compass design study shows that a PPE class high power SEP vehicle enables payload delivery of masses that inversely vary with the trip time desired to arrive at Mars. One of these payloads could be a high-power communications package. With its high-power solar arrays and efficient SEP system, a PPE class system could function as a long duration highly capable Mars communications relay satellite.

---

[1] Melissa L. McGuire, Steven L. McCarty, Daniel J. Grebow, Thomas A. Pavlak, Scott N. Karn, Kaushik S. Ponnapalli, Diane C. Davis, and Kurt J. Hack, "Overview of the Lunar transfer trajectory of the co-manifested first elements of NASA's Gateway," 2021 AAS/AIAA Astrodynamics Specialist conference, Aug 8-12, 2021

[2] M. McGuire, S. McCarty, K. Hack, S. Karn and D. Davis, "Application of Solar Electric Propulsion to the Low Thrust Lunar Transit of the Gateway Power and Propulsion Element" *38th International Electric Propulsion Conference*, Toulouse, 2024.

[3] Melissa L McGuire, Steven R, Oleson and Timothy R. Sarver-Verhey, "Concurrent Mission and Systems Design at NASA Glenn Research Center: The Origins of the COMPASS Team," Space 2011 Conference and Exposition, Sept 27-29, 2011.

[4] Elizabeth Turnbull, Melissa McGuire and Steven Oleson, "Lessons Learned in Concurrent Mission and Systems Design at NASA Glenn Research Center: Almost Fifteen Years of the Compass Team," 9th International Conference on Systems & Concurrent Engineering for Space Applications (SECESA). Sept 2020.

[5] NASA Launch Services Program, Launch Vehicle performance Website. http://elvperf.ksc.nasa.gov/Pages/Default.aspx, April 11, 2025

[6] **HT-6000** High power. High Performance, https://www.busek.com/bht6000, Dec 04,2025

[7] S. Karn, S. McCarty, and M. McGuire, "Analysis of Cislunar Transfers Departing from a Near Rectilinear Halo Orbit Using Solar Electric Propulsion", AAS/AIAA Astrodynamics Specialist Conference, Virtual, 2021.

[8] Copernicus Trajectory Design and Optimization System**,** https://www.nasa.gov/general/copernicus/, Dec 04,2025

[9] Williams, Jacob, "Copernicus Spacecraft Trajectory Design and Optimization Program," FortranCon 2020, July 2, 2020.

[10] Optimal Trajectories by Implicit Simulation (OTIS) Version 5.0: A General Purpose 3-DOF Aerospace Vehicle Trajectory Simulation and Optimization Computer Program (LEW-20403-1) https://software.nasa.gov/software/LEW-20403-1, Dec 04,2025

[11] Daniel Herman, T Gray, I Johnson, S Hussein, and Taylor Winkelmann, "Development and Qualification Status of the Electric Propulsion Systems for the NASA PPE Mission and Gateway Program", IEPC-2022-465 *Presented at the 37th International Electric Propulsion Conference*, *Boston, MA, United States*, *June 19 – 23, 2022*

[12] J. Jackson, S. Miller, J. Cassady, E. Soendker, B. Welander, M. Barber and P Peterson, "13kW Advanced Electric Propulsion Flight System Development and Qualification", *36th International Electric Propulsion Conference*, 2019

[13] Laura M Burke, Steven R Oleson, Zachary C Zoloty, David A Smith, and Maya N Havens, "Combined 1-MW Solar Electric and Chemical Propulsion for Crewed Mars Missions," AIAA ASCEND (Accelerating Space Commerce, Exploration, and New Discovery, Las Vegas, NV, Oct 23, 2023.